Efficient Carrier Acquisition and Tracking for High Dynamic and Weak Satellite Signals

Xiang Gao[1], Yong Li [1], and Jianrong Bao[2]
[1] School of Electronic and Information, Northwestern Polytechnical University, Xi'an, 710072, P.R. China
[2]School of Communication Engineering, Hangzhou Dianzi University, Hangzhou, 310018, P.R. China
Email: gaoxiang6175@mail.nwpu.edu.cn; ruikel@nwpu.edu.cn; baojr@hdu.edu.cn

Abstract —Under high dynamic and weak signal environment in the satellite Tracking, Telemetry and Command (TT&C) systems, the carrier acquisition and tracking can't be easily achieved. In this paper, an improved two-stage high dynamic and weak signal carrier acquisition and tracking are presented for perfect carrier synchronization. The typical U.S. Jet Propulsion Laboratory (JPL) high dynamic carrier model is adopted here to develop the proposed carrier acquisition and tracking performance. In the first stage, the fast Fourier transformation (FFT) based cyclic shifting accumulation periodogram carrier acquisition method is proposed to obtain the coarse carrier frequency offsets as well as the Doppler rate efficiently and quickly. In this procedure, the replacement of the time domain multiplication with the frequency domain cyclic shifting is proposed for low complexity. Also a variable rate sampling is adopted for better accuracy of FFT carrier spectrum calculation. In the second stage, a second-order Frequency Locked Loop (FLL) assisted by a third-order phase locked loop (PLL) is proposed to correct the residual carrier frequency and phase offsets and achieve a much fine carrier recovery. In these two stages, the structure of the proposed algorithm is also analyzed for optimal synchronization parameter selection. The simulation results show that the proposed carrier acquisition and tracking method performs efficiently under a high dynamic and low Signal-to-Noise Rate (SNR) environment for the satellite transmission applications. Therefore, the proposed carrier synchronization method is quite pragmatic and it can be effectively applied in the high dynamic and low SNR satellite communications with high efficiency and low complexity.

Index Terms—High dynamics, carrier recovery, carrier acquisition, carrier tracking, FFT, FLL, PLL

I. INTRODUCTION

In the satellite TT&C systems, especially for the Low-Earth-Orbit (LEO) satellites, there are large relative speed and acceleration phenomena between the satellites and the ground stations. They cause the high dynamic Doppler phenomenon, including the Doppler frequency and Doppler rate, *i.e.* the acceleration of the Doppler frequency, which degrade the satellite signal reception at the ground stations [1]. And the long distance between the satellite and the station also results in low SNR transmission environment, which further deteriorates the signal detection in the ground station receivers. So the signal receptions in the satellite communications are confronted with the challenge of the carrier synchronization, especially for the high dynamic and weak satellite communication signals.

Traditionally, carrier synchronization was performed by two stages of the carrier acquisition and tracking [2]. The research statuses of them were as follows.

(1) For the carrier acquisition, *i.e.* the coarse estimate of the Doppler frequency and Doppler rate, it can be implemented by the linear prediction based frequency estimation [3]. But it was suffered from large acquisition latency and it can't work efficiently at low SNRs. Also the satellite receiver can't detect and demodulate the satellite signals in real time easily under the high dynamic environments. Accompanied with the development of the FFT technology, modern signal processing and the digital signal processor, FFT based practical frequency domain carrier acquisition occurred [2]. By the frequency domain analysis of the time domain correlated integrations, the instantaneous carrier frequency can be located to achieve fast carrier acquisition and it assisted the successive carrier tracking [4]. Then, there were mainly three classes of the classic carrier acquisition algorithms, such as the maximum likelihood (ML) estimation [5], the Cross-Product Automatic Frequency Control (CPAFC) [6], [7], the extended *Kalman* filter (EKF) and the improved methods [8], [9], which had been applied in the Mar exploration rovery entry [10]. They were also analyzed and compared in [11], [12]. ML estimation algorithm can obtain a fine estimation of the frequency and phase at the cost of highest computational complexity and very poor real-time capability. Also an improved ML method for the joint estimation of the Instantaneous Frequency (IF) and Instantaneous Frequency Rate (IFR) was proposed to reduce two-dimensional grid search as one dimension for low complexity. But there was little loss of accuracy [13]. The CPAFC algorithm was a negative feedback working system by the frequency discriminator. It was easily limited by the loop bandwidth and was difficult to work efficiently for both the dynamic property and low-SNR. EKF algorithm approximately processed the nonlinear parametric equations linearly, and it iteratively estimated

Manuscript received March 4, 2016; revised July 16, 2016.
This work was supported by the Zhejiang Provincial Natural Science Foundation of China (No.LZ14F010003), the National Natural Science Foundation of China (No.61471152), the Open Research Fund of National Mobile Communications Research Laboratory, Southeast University (No.2014D02) and the Zhejiang Provincial Science and Technology Plan Project (No.2015C31103)
Corresponding author email: gaoxiang6175@mail.nwpu.edu.cn.
doi:10.12720/jcm.11.7.644-652

the current state by input signals with high estimation accuracy. But the high complexity of the implementation led to the difficulty of very high speed computation. Furthermore, EKF method estimated the signal phase and it had quite slow convergence rate, as well as the narrow acquisition range. In short summary, among the above three classes of the carrier acquisition algorithm, the ML estimation algorithm was the most proper method suited for the high dynamic and low SNR environment in satellite communications. But it still needed to be further optimized for low complexity in practice. Besides the above three basic algorithms, there were also modified carrier acquisition method. In [10], a new carrier acquisition method was proposed as the multiple path time domain change rate matching and the maximum of the FFT calculation module, which captured the Doppler frequency and the first-order Doppler rate. But it required much accurate matching of the time domain change rate. So it needed huge quantity of the matching paths, which resulted in the enormous computation, which restricted it from application in practice. In [11], a periodogram based ML algorithm was proposed to reduce the matching accuracy requirement of the Doppler rate and thus cut down the computational complexity, which had been used in Mar exploration. Also some effort to further reduce the complexity about this algorithm had been done in [12]. But the performance had degraded a little. Then, an Adaptive Line Enhancer (ALE) was applied before the FFT acquisition to improve the acquisition performance and reduce the acquisition time [14]. And the output SNR and the dynamic detection ability were also enhanced.

(2) For the carrier tracking, once the large carrier frequency offset was estimated and compensated, the mature FLL-PLL technique [2] can be adopted to not only exploit the FLL accommodation ability for high dynamics signals, but also take advantage of the PLL for the high tracking phase accuracy. They obtained good performance by careful loop parameter design. With the development of carrier synchronization, they had also been implemented in the QPSK software defined radio [15] and SOQPSK satellite modem [16] efficiently.

According to the above analysis of the existing carrier acquisition and tracking algorithms for high dynamic and weak signals in satellite communications, we further analyze the principle of the periodogram based carrier capture algorithm and adjust the coherent accumulation of the FFT based segment periodogram calculation to improve the acquisition performance. So in this paper, the FFT base frequency-domain cyclic shifting Periodogram accumulation algorithm is proposed to simplify the coarse carrier acquisition in the first stage. Then, in the second stage, the CPAFC based FLL-PLL structure is applied for precise tracking of the small residual Doppler frequency and Doppler rate by compensating them. And in the FLL-PLL structure, a second-order CPAFC carriier tracking structure [7] is designed, followed by a third-order PLL structure, which had been analyzed for the optimized phase lock and tracking performance [17]-[19].

The paper is organized as follows. Section II describes the baseband equivalent high dynamic signal model. In Section III, the improved FFT based by frequency-domain shifting accumulation is proposed and analyzed for its acquisition accuracy and computational complexity. Then, the joint FLL-PLL with pre-compensation of Doppler rate is given to improve traditional tracking algorithms in Section IV. In Section V, the simulation shows that the proposed joint frequency recovery obtains a precise acquisition and tracking of the carrier frequency under extremely low SNR and high dynamic environment. Finally, conclusions are given in Section VI.

II. System Diagram and Doppler Signal Model

In this paper, a hierarchical carrier offset estimation and adaptive compensation algorithm is employed, where the FFT frequency domain coarse carrier acquisition is performed and compensated before the fine FLL-PLL carrier tracking. The block diagram of a general carrier acquisition and tracking is shown in Fig. 1.

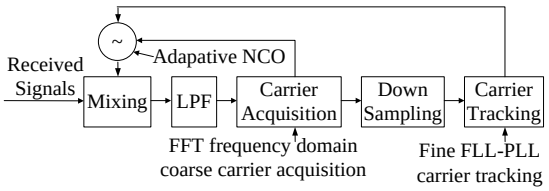

Fig. 1. General carrier acquisition and tracking block diagram

The frequency of the baseband equivalent signals received in the satellite ground station includes the Doppler frequency, Doppler rate and even much higher order frequency change rate. Similar to the analysis in [12], the signal frequency can use the first-order constant acceleration model based on the high dynamic motion model of Jet Propulsion Laboratory (JPL). So for a QPSK modulation system, the received complex baseband signal $r(t)$ is expressed as

$$r(t) = A \cdot e^{j[2\pi(f_c + f_d)t + \pi a t^2]} + n(t) \quad (1)$$

where A is the information bit to be modulated and transmitted with the value of "1" or "-1", f_c, f_d and a are the ideal carrier frequency, the Doppler frequency and the Doppler rate, $n(t)$ is the complex additive white Gaussian noise (AWGN) with mean 0 and variance σ^2 (*i.e.* $n(t)$~N(0, σ^2)). The Doppler parameters of f_d and a are required to be accurately estimated and compensated in the carrier synchronization algorithm.

In practice, the signal is sampled at the receiver and the algorithm can be processed digitally. Suppose there are N samples in a given time slot T, the sampled signal $r(n)$ from (1) can be expressed as

$$r(n) = Ae^{j[2\pi(f_c + f_d)Tn/N + \pi a T^2 n^2/N^2]} + n_d(n) \quad (2)$$

where $n_d(n)$ is the sampled AWGN $n(t)$ in (1). Given the local complex carrier $\exp(-j2\pi f_c Tn/N)$ from the adaptive Numerical Control Oscillator (NCO) in Fig. 1, the output signal after mixing and low pass filtering is given as

$$\begin{aligned} r'(n) &= r(n)\cdot e^{-j2\pi f_c Tn/N} \\ &= A\cdot e^{j[2\pi f_d Tn/N+\pi aT^2n^2/N^2]} + n_d(n)\cdot e^{-j2\pi f_c Tn/N} \\ &= A\cdot e^{j[2\pi f_d Tn/N+\pi aT^2n^2/N^2]} + n_{dn}(n) \end{aligned} \quad (3)$$

where $n_{dn}(n)$ is also the AWGN, except that the sampled AWGN $n_d(n)$ is shifted in frequency by f_cT/N.

Due to the large initial carrier frequency offsets, the bandwidth of the Low Pass Filter (LPF) in Fig. 1 should be greater than the maximum carrier frequency and allow most energy pass of the carrier signals. But it also brings much noise into the filtered signals, which requires that the algorithm can work at low SNRs.

Then in the carrier acquisition, the Doppler frequency and Doppler rate are searched in two dimensions of their possible range and the estimates of them are compensated for the small residual carrier offsets in the receiver, which obtains rather good carrier tracking performance by the traditional FLL-PLL based method and accomplishes the complete carrier synchronization. Meanwhile, before the carrier acquisition and tracking, the signal frequency is very large and it greatly increases the calculation burden. So the signals should be down sampled by a decimator at first to reduce the computation burden.

III. Improved Periodogram Shifting Accumulation Algorithm for Coarse Carrier Acquisition

The carrier of the above mentioned signal with carrier offsets can be coarsely captured by the FFT frequency based periodogram method [20]. Firstly, we just consider a pure signal $r_p(n)$ after the mixing and the low pass filtering in (3) without noise contamination and it is $A\times\exp[j(2\pi fdTn/N+\pi aT^2n^2/N^2)]$. Having a FFT on each data $r_p(n)$ and calculating and averaging the square of the module of the FFT computations, the final result of the periodogram algorithm is expressed as follows.

$$\begin{aligned} P(f_k) &= \sum_{all\ n} |FFT[r_p(n)]|^2 \\ &= \sum_{all\ n} |A\sum_{n=0}^{N-1} e^{j[2\pi f_d Tn/N+\pi aT^2n^2/N^2+\theta_0]} e^{-j2\pi kn/N}|^2 \\ &= \sum_{all\ n} |A\sum_{n=0}^{N-1} e^{j2\pi n/N[f_dTn+aT^2n^2/(2N)-k]} e^{j\theta_0}|^2 \end{aligned} \quad (4)$$

where θ_0 is the phase offset caused by the oscillators between the transmitter and receiver. So the possible estimates of the Doppler parameters are compensated into the intermediate signal $r'(n)$. Then, f_d and a are calculated by the optimization equation as follows.

$$(f_{d,opt}, a_{opt}) = \arg\max_{(f_d,a)}[P(f_k)] \quad (5)$$

In the above optimization Eq. (5), the relationship of $P(f_k)$ with the carrier frequency parameters of f_d and a is the key to solve the optimization. From (4), it is obvious that the maximization of $P(f_k)$ can be obtained when the Doppler parameters of f_d and a are compensated by the k and the exponent item $[f_dTn+At^2n^2/(2N)-k]$ approaches to 0 as close as possible.

Under low SNR environment, the bandwidth of the carrier tracking system is usually very narrow. This also requires the narrow bandwidth of the frequency change rate of the signal to be demodulated. In order to capture the carrier of large frequency change rate, the possible occurred dynamic range of the Doppler frequency and rate should be divided for several segments. In the algorithm, the Doppler frequency and the first-order derivation of it are considered. The Doppler frequency and rate can be divided into several ranges for the two dimensional searching of their optimal estimates. And the possible searching range of the Doppler rate is set as $[a_{\min}, a_{\max}]$. Each input signal for the carrier acquisition will be multiplied by the preset Doppler frequency rate. When the Doppler frequency rate in one branch closely approaches the true Doppler rate, the maximum average periodogram peak occurs. And the estimated Doppler rate can be obtained. So in each divided branch, the frequency change rate of the signals can be recognized as negligible. And the carrier acquisition can be carried out in each segment with FFT computation in (4) and the estimates of the Doppler parameters are obtained by the maximization of $P(f_k)$. So according to the above two dimensional searching of the periodogram algorithm, the received signal after the mixing and LPF can be divided into M continuous sub-data segment for separate periodogram calculation and each of them sustains for $\Delta T=T/M$.

After N samples (equivalently after the T second), the successive cycle of the intermediate signal $r'(n)$ in (3) is expressed as follows.

$$\begin{aligned} r'(n+N) &= A\cdot e^{j[2\pi f_d T(n+N)/N+\pi aT^2(n+N)^2/N^2]} + n_{dn}(n+N) \\ &= C_N\cdot s(n)\cdot e^{j2\pi anT} + n_{dn}(n+N) \end{aligned} \quad (6)$$

where C_N is represented as

$$C_N = A\cdot e^{j2\pi[f_dT+aT^2/2]} \quad (7)$$

which is a constant independent of n. Then, the FFT of the signal is expressed as

$$R'(k) = C_N\cdot S(k-aT) + N_{dn}(k) \quad (8)$$

According to the above analysis, the two dimensional periodogram frequency acquisitions with FFT frequency domain shifting accumulation can be listed as follows.

Since the nature of the carrier acquisition is the searching in the value space of the Doppler frequency and rate, a total of M Doppler frequencies and R Doppler rates are carried out for the optimal carrier estimation. So the signal $r_p(n)$ is multiplied by R Doppler rates in the range and the final signal $x_l(n)$ is expressed as

$$x_l(n) = r_p(n)\cdot\exp[-j\pi a_l T^2n^2/N^2] \quad (9)$$

where a_l $(1\le l\le R)$ represents the l-th supposed carrier frequency rate in the searching range. After multiplication, the sequence $\{x_l(n)\}$ is divided into M continuous sub-data segments with time interval $\Delta T=T/M$. Then, each sub-data segment is calculated by the FFT. So the squared amplitude of each FFT result is calculated for

mean value and the estimate $P(f_k)$ of the periodogram can be calculated by the accumulation of all these square of the FFT results. The parameter in the calculation of $P(f_k)$ is as follows: $1 \le l \le R$, $f_k = k/\Delta T$, $-R/2+1 \le k \le R/2$. Finally, the estimates of the Doppler frequency and rate, *i.e.* the solution in optimization equation (5), can be obtained by searching the maximum $P(f_k)$.

In addition, the algorithm can be further improved for low complexity. Two measures of the improvement can be the variable sampling and the replacement of time domain multiplication by the frequency domain cyclic shifting. They are described as follows.

1) Variable rate sampling.

In the above analyses, the proposed carrier acquisition works under low SNR and high dynamic environment. But the sampling before FFT calculation in the algorithm is fixed, which leads to some problems. Suppose the Doppler rate is a constant in the searching range, the preprocessed signal $r'(n)$ for carrier acquisition in (3) is.

$$r'(n) = A \cdot e^{j[2\pi f_d Tn/N + \pi a T^2 n^2/N^2 + \theta]} + n_{dn}(n) \quad (10)$$

where a is a constant and θ is the phase offset. If the fixed sampling is adopted, the variation of the carrier phase will be nonlinearity of the high order of acceleration due to the change of frequency change rate. So the phase offsets between the adjacent sampling points are time variant. At this moment, the frequency distribution of the FFT of these signal samples is very hard to be converged on a narrow range and they will scatter at a rather wide region. And this phenomenon is the so called platform effect, which has a great influence in the carrier acquisition decision. The fixed rate sampling method results in a spread of the estimated frequency since it will not compensate the sampling offset caused by frequency errors. However, the sampling rate can also be adjusted to reduce the phenomenon to a large extent. By the variable rate sampling, it can adjust the sampling rate exactly suited to the ideal and most proper samples for estimation. And the corresponding variable sampling rate method is proposed and analyzed as follows.

The sampled signal $r(n)$ in (2) is used here for variable rate sampling analysis. The sampling frequency and signal carrier frequency are f_s and f_c. Assume the precondition $f_s >> f_c$, the signal frequency can be approximately considered as invariant. At the time instance $n=0$, the initial digital phase offset $\Delta\theta(0)$ is

$$\Delta\theta(0) = f_c T_s(0) = f_c / f_s(0) \quad (11)$$

where $T_s(0)$ and $f_s(0)$ are the initial sampling period and frequency at time instance 0. At other time instance $n<N$, the normalized digital phase offset $\Delta\theta(n)$ is

$$\Delta\theta(n) = f(n) T_s(n) = (f_c + anT/N) / f_s(n) \quad (12)$$

where $f(n)$ is the instantaneous frequency of the moment n. Given the precondition that the phase offset at each sampling is a constant, there is

$$(f_c + anT/N) / f_s(n) = f_c / f_s(0) \quad (13)$$

After simple transform of (13), there is

$$\begin{aligned} f_s(n) &= f_s(0) + f_s(0) \cdot anT/(Nf_c) \\ &= f_s(0) + k' \cdot n \end{aligned} \quad (14)$$

where k' is the constant coefficient in the second item and it is the variable factor to be used in the variable sampling.

So the normalized digital frequency can be obtained. When the precondition ($f_s >> f_c$) is not satisfied, the normalized digital frequency can also be obtained, which can be analyzed as follows.

Suppose the adjacent sampling moment m and $m+1$, the phase difference in this time interval is

$$\sum_{n=m}^{n=m+1} f_s(n) = \Delta_1\theta \quad (15)$$

Based on (14) and (15), we can get the phase offset due to the sampling and it is given as

$$f_s(0)T + 1/2 \cdot k'T^2 + k'mT^2/N = \Delta_1\theta \quad (16)$$

And the phase offset by the signal is calculated as

$$\Delta_2\theta = \sum_{n=m}^{n=m+1} f(n) = f_c T + \frac{1}{2}aT^2 + \frac{1}{N}amT^2 \quad (17)$$

In order to get the same phase offset between (16) and (17), *i.e.* $\Delta_1\theta = \Delta_2\theta$, the variable factor to be used in the variable sampling is as follows.

$$k' = f_s(0) / f_c \cdot a \quad (18)$$

Finally, we have a numeric verification about the effect of the fixed and the variable rate sampling of the FFT calculation of the signals with carrier frequency offset. For the fixed sampling, the simulation parameters are as follows: f_c=1kHz, k'=1kHz/s, f_s=20kHz. For the variable sampling, f_c=1kHz, $k' = f_s(0)/f_c \cdot a$=4kHz/s, $f_s(0)$=4kHz. Then, the simulation is shown in Fig. 2.

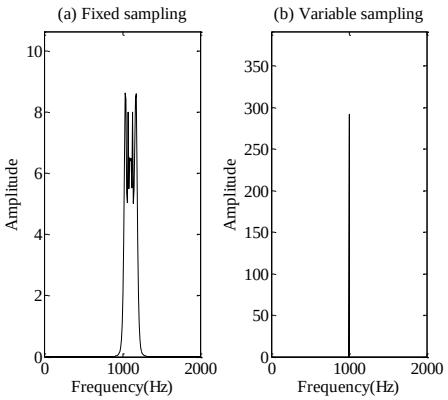

Fig. 2. Amplitude-frequency response of the periodogram algorithm with the fixed and variable rate sampling

From the fixed rate sampling method shown in Fig. 2 (a), the maximum amplitudes occur not only in the true frequency offset f_c=1kHz, but also persists for a rather wide range from 1kHz to 1.3 kHz, which deteriorates the performance of the frequency estimation. But from the improved variable rate sampling method shown in Fig. 2 (b), the maximum amplitudes concentrate on a very narrow band around the true frequency offset f_c=1kHz,

which greatly improves the possible carrier acquisition with high resolution. In addition, it not only removes the frequency spread platform effect, but also has higher amplitude response, almost 30-40 times of the former contrast fixed rate sampling method, which helps improve the carrier acquisition a lot.

2) Replacement of the time domain multiplication with the frequency domain cyclic shifting.

In the periodogram carrier acquisition algorithm, the input signals are multiplied by the preset Doppler frequency change rates in each branch. When the Doppler frequency change rate in one branch closely approaches the true one, there will be a maximum of the average accumulation of the periodogram algorithm. The location in the maximum value is the estimated frequency. And the preset Doppler change rate is the optimal estimation of itself. In this process, the multiplication of the received signal with a Doppler frequency change rate is followed by the FFT computation. So it can be improved for low complexity as follows.

Due to the property that a signal multiplied by a rotate factor is equivalent to the signal in frequency domain with a shift of frequency [20], the FFT cyclic shifting accumulation algorithm is employed to eliminate the multiplication of the pre-compensation of the possible frequency offset in the search algorithm.

Faced with the different Doppler rate, the FFT of the signal in the same time span can be obtained by the cyclic shifting FFT of the signal in the initial time span at a different rate *aT*. Consequently, the compensation to the signal Doppler rate can be accomplished by the shifting of the digital frequency of signal in reverse direction at a different rate. Finally, the schematic of the proposed carrier acquisition is shown in Fig. 2.

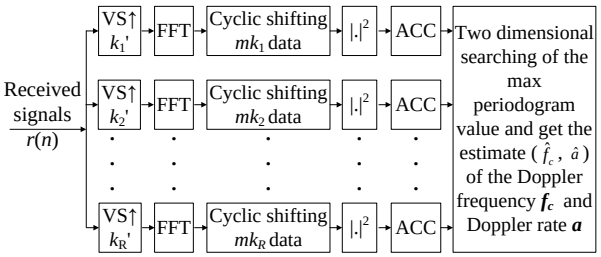

Fig. 3. FFT frequency shifting accumulation periodogram algorithm for coarse carrier acquisition. The term "VS" and "ACC" in the figure stand for "variable rate sampling" and "accumulation", respectively

In Fig. 3, m=1, 2,⋯, M, the cyclically shifting number k_1, k_2, …, k_R in every matching branch are correspond to the Doppler rate estimation a_1, a_2, …, a_R for the local carrier frequency acceleration. R is the number of the branches. Assuming the sampling frequency f_s as the total number of the sampling points at each time instance T, there is the following relationship of

$$k_R = a_r \cdot N^2 / f_s, r = 1, 2, \cdots, R \tag{19}$$

After M branches of FFT calculation with average and accumulation, the amplitude in the i-th branch may get the maximum value and the corresponding preset a_i is the Doppler rate estimation. The peak point is the prediction of the frequency offset Δf, and the initial carrier frequency is obtained as $f_c+\Delta f$. If the amplitude of the peak point is larger than the preset threshold, the carrier frequency acquisition is successful. Otherwise, the searching is failed and no carrier is captured. And the threshold should be decided by the real transmission situations in order to avoid the false carrier capture mainly caused by random noise, which is used to reduce the false alarm probability of the carrier acquisition.

The M branch of FFT calculation and maximum peak point searching are carried out parallel for high efficiency and the complexity of the N points FFT calculation is also reduced as the M times of N/M points FFT calculation.

In practice, the algorithm may encounter the situation where k_i is not an integer and the rounding operation will affect acquisition performance. To solve the problem, some zeros are often padded to the sampling data for l times before the FFT computation. Compared with the carrier acquisition algorithm proposed in [10], the proposed algorithm obtains similar acquisition accuracy and acquisition probability, as well as the computational complexity reduced by l times. Assuming that N is the number of the FFT points, the frequency estimation satisfies $f_{dres}<f_s/N$ and the Doppler rate estimation satisfies $a_{dres}<(a_{max}-a_{min})/l/2$ after the completion of the coarse carrier acquisition. The acquisition probability is up to 96 %. The output signal of the local NCO after completion of carrier acquisition is expressed as

$$S_{NCO}(n) = e^{j[2\pi f_{dres} Tn/N + \pi a_{res} T^2 n^2/N^2 + \theta]} \tag{20}$$

where θ is the initial phase offset.

IV. Joint CPAFC Based FLL and PLL Carrier Tracking Loops for Fine Carrier Tracking

After the completion of coarse carrier acquisition, the carrier tracking loop for fine carrier synchronization is carried out with all Doppler frequency and Doppler rate are compensated in the first stage. And the schematic block diagram of the carrier tracking is shown in Fig. 4.

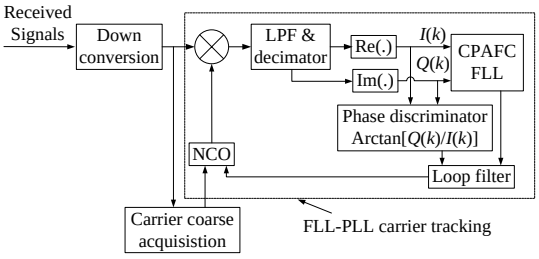

Fig. 4. Joint CPAFC FLL-PLL algorithm for fine carrier tracking.

FLL can reach lower tracking threshold compared with PLL, which is suited for weak signal demodulation. It has better resistance against high dynamics and interference. But it has rather large frequency estimate errors. On the contrary, PLL can reach high tracking accuracy but it is

very sensitive to the large dynamics and interference. Consequently, the PLL is turned on to track carrier once the FLL tracking is locked. This scheme not only improves the tracking robustness, but also improves the tracking accuracy. When the former coarse carrier acquisition is completed and compensated, the successive frequency signal still has residual Doppler frequency and Doppler rate. So a second-order FLL assisted third-order PLL is used here as the carrier tracking to make sure no steady-state carrier phase errors in the demodulation.

After completion of carrier acquisition, the baseband signal entering carrier tracking module is indicated as

$$r_{acq}(n) = A \cdot e^{j[2\pi f_{dres} Tn/N + \pi a_{res} T^2 n^2 / N^2]} + n_{dnres}(n) \quad (21)$$

where f_{dres} and a_{res} are the residual Doppler frequency and the Doppler rate after coarse carrier compensation, $n_{dnres}(n)$ is also the output noise, which can be generated by a sampled AWGN passing through the coarse carrier acquisition and compensation module, and it can be modeled as the narrow band AWGN within the signal bandwidth range. The aim of the carrier tracking is the completion of the precise estimation of f_{dres} and a_{res} to guarantee the good carrier demodulation performance. From Fig. 4, the orthogonal signals $I(k)$ and $Q(k)$ after LPF & decimator module can be expressed as

$$\begin{aligned} I(k) &= A\cos[2\pi(f_{dres} + a_{res} kT'/2)kT'] \\ Q(k) &= A\sin[2\pi(f_{dres} + a_{res} kT'/2)kT'] \end{aligned} \quad (22)$$

where T' is the inverse of the sampling frequency after down sampling.

Meanwhile, the output of the cross-product frequency discriminator (FD) is approximately calculated as

$$\begin{aligned} \Delta f_{FD} &= I(k-1)Q(k) - I(k)Q(k-1) \\ &= \sin\{2\pi[f_{dres} + a_{res}(2k+1)(T_s')^2/2]\} + n_{\Delta f_{FD}} \\ &\approx 2\pi[f_{dres} + a_{res}(2k+1)(T_s')^2/2] + n_{\Delta f_{FD}} \end{aligned} \quad (23)$$

where $n_{\Delta fFD}$ is the noise brought by the CPAFC loop.

And the output of the phase discriminator (PD) is

$$\Delta f_{PD} = 2\pi[f_{dres} + a_{res} kT'/2]kT' + n_{\Delta f_{PD}} \quad (24)$$

where $n_{\Delta fPD}$ is the noise brought by the PLL loop.

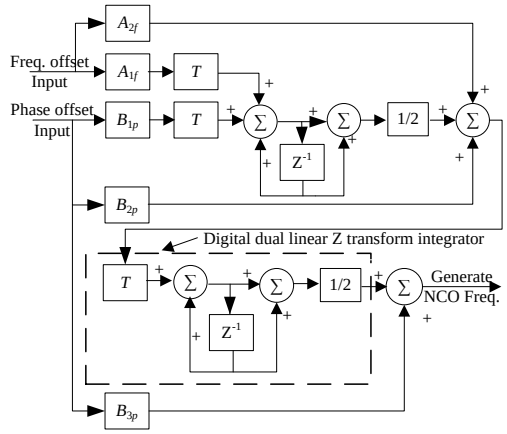

Fig. 5. Carrier tracking loop of 2nd-order FLL with 3rd-order PLL.

When the residual Doppler rate a_{res} isn't equal to 0, the result of the FD in the CPAFC-FLL is the linear function interfered by the noise with the slop. And the output of the PD in the PLL is the second parabolic function interfered by the introduced noise too.

Based on the above analyses, the joint second-order FLL aided third-order PLL can be designed in Fig. 5.

If the loop bandwidth is properly chosen, the difference between the ideal and practical carrier tracking threshold is very small. One instance of the loop parameters in the FLL and PLL are shown in Table. I. The parameters of w_f and w_p are the natural circular frequency of the loop filters and valued 17.45 and 22.27, respectively.

TABLE I: LOOP PARAMETERS OF THE FLL AND PLL

Loops	Noise bandwidth (Hz)	Loop coefficients
2nd-order FLL	B_f=0.58w_f=10.12	A_{1f}=w_f^2=102.41, A_{2f}=1.414w_f=27.77
3rd-order PLL	B_p=0.82w_p=18.26	B_{1p}=0.1w_p^3=1104.49, B_{2p}=1.12w_p^2=555.46, B_{3p}=2.4w_p=53.45

In the normal fine carrier tracking, the loop bandwidth B_{PLL} must be set to a very small value to get high tracking accuracy. And only very small carrier Doppler rate can be tolerated by the loop, otherwise it may be out of locking and fail to track the carrier. So the Doppler rate should be corrected a lot in the FLL and the B_{PLL} must be set to a rather large value initially until the carrier frequency is locked well. Also a preceded coarse carrier acquisition should be adopted to correct most of the carrier frequency errors and then the carrier track can perform well.

V. NUMERICAL SIMULATION AND RESULT ANALYSES

To verify the effectiveness of the proposed carrier acquisition and tracking algorithm, the estimates of the frequency and phase are simulated and compared with the corresponding ideal carrier parameters. And the results of carrier acquisition and tracking are as follows.

In the first stage of coarse carrier acquisition, two dimensional searching of the Doppler frequency and Doppler rate are based on the 8 segment parallel search of the max amplitude by the periodogram algorithm. The signal model for simulation is established as all digital sampling in (2). The step of the Doppler rate is 20Hz/s in each branch of searching with totally 32 branches. After down sampling, the signal sampling frequency of each frequency segment is 800 kHz. The Monte Carlo simulation of 2000 times is executed in the coarse carrier acquisition according to the carrier acquisition block diagram in Fig. 2.

Firstly, we check out the performance of the proposed algorithm at different SNRs, especially at very low SNRs. The experiment parameters are as follows. The data rate is 10 kbps, the carrier offset is 1kHz, the number of total simulation points is 10^6, the initial sampling rate is 4kHz and the coefficient of the variable step of the sampling, *i.e.* k' in (14), is 0.2. The amplitude of the periodogram

algorithm is calculated at SNR of 0dB and -20dB, respectively. The 2048 point FFT computation is adopted and the resolution ratio of the spectrum analysis is $f_s(0)/N$, *i.e.* 4k/2048=2Hz, at first and then it is increased with the variable step sampling rate described in (14), Then, after FFT transformation, the spectrum of the signals at SNR of 0dB and -20dB are shown in Fig. 6 (a)&(b), respectively.

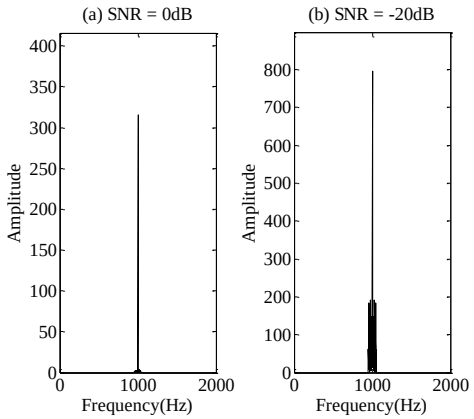

Fig. 6. The output amplitudes of FFT spectrum at different SNRs.

From Fig. 6, larger noises in the received signals result in the phenomena of more false estimated amplitude of the FFT spectrum near the optimal estimate of frequency offset. And it can be explained by the periodogram algorithm in equation (4) by adding a noise item in the received signal $r_p(n)$. Since the square operation of the true signal added by a noise, there will be the two items of the true signal multiplied by a noise and the square of the noise in the true periodogram power spectrum. So the effect of the noise influences the estimation resolution of the amplitude of the FFT spectrum. Then, at different SNRs as 0dB and -20dB, the peaks of the amplitude of FFT spectrum all occur at the actual frequency point of 1 kHz in Fig. 6. So by the proposed two-dimensional carrier acquisition algorithm, the carrier can be captured at extremely low SNRs, *i.e.* as low as -20dB. So the proposed carrier acquisition can be used in the satellite system under high dynamic and low SNR environment efficiently.

Finally, the simulation is carried out with the above parameters and the proposed carrier acquisition algorithm, the acquisition result is shown in Table. II.

TABLE II: ACQUISITION RESULTS BASED ON THE FFT FREQUENCY SHIFTING ACCUMULATION PERIODOGRAM ALGORITHM

Item	value
Date rate(kbps)	10
E_b/N_0/(dB)	1
Segment number	8
FFT points number	2048
Doppler rate/(Hz/s)	-320 to 320
Doppler frequency/(kHz)	-2.4 to 2.4
Doppler rate estimation accuracy/(Hz/s)	±10
Doppler frequency estimation accuracy/(Hz)	±20

In Table II, the proposed carrier acquisition algorithm obtains rather good performance with high resolution of carrier acquisition. And it can work at a broad range of Doppler frequency and rate with low residual estimation errors, which makes it very pragmatic in practice.

In the second stage of carrier tracking, the traditional FLL-PLL loop and proposed tracking loop in Fig. 4 is adopted to perform the carrier tracking simulation. The experiment parameters are as follows. Total 2×10^4 points are simulated in the carrier tracking system. The data rate is 10kbps, the maximum of the absolute value of the frequency offset is 300kHz, the initial Doppler frequency offset is also 300kHz and the absolute value of the frequency accelerate rate is 30kHz/s. With the above parameters, the relationship between the final instantaneous frequency error and the varying time is shown in Fig. 7, where the residual frequency tracking offsets, the Frequency offsets by frequency acceleration (mainly tracking and compensating the Doppler rate) and the residual phase tracking offsets are displayed.

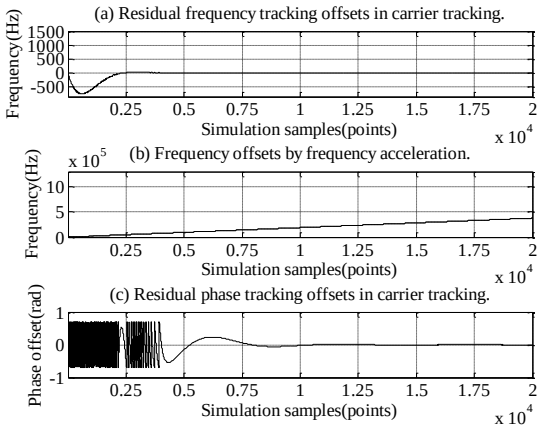

Fig. 7. Frequency/phase tracking effect in proposed FLL-PLL loop

In Fig. 7(a), the carrier frequency offset is very close to zero at the simulation sample point 2500, which indicated that the frequency tracking is locked. At the same time, shown in the 7(b), the Doppler rate is well tracked and the slope of the curve is almost constant, which solves the Doppler rate. So after this moment, the carrier frequency is well locked and eliminated. From Fig. 7(c), the carrier phase offsets by the proposed tracking method has been eliminated almost to zero at the simulation sample point of 10^4, which shows a good carrier phase tracking performance. In this procedure, the carrier phase can be tracked well until the accurate carrier frequency tracking is achieved. So the stabilization of the phase offset should be later than that of the frequency offset.

Under the same experiment parameters, the second-order FLL and third-order PLL all can't track the high dynamic signals separately. The PLL can't track rather large frequency acceleration, while the FLL can only track frequency offset, but it can't track carrier phase. However, they are complementary and can jointly track the high dynamic carrier signal cooperatively. At the same time, if there are rather large initial carrier frequency and phase offsets, it costs much time to finish the tracking the carrier. So the coarse carrier acquisition

can help reduce the residual carrier errors for the fast tracking in the second stage. Therefore, the two-stage carrier acquisition and tracking must be optimized together for much lower complexity and less latency, which is required in practice.

The computational complexity of the proposed carrier acquisition and tracking algorithm decreases a lot when compared with that in Ref. [10], since the reduction of multiply operation before the FFT calculation replaced by the equivalent cyclic shifting of the data after FFT computation. Given the *N*-point FFT calculation, the corresponding reduction of the computational complexity can be listed in Table. III as follows.

TABLE III: COMPARISON OF COMPUTATIONAL COMPLEXITY

Method	Complex Multiplications	Complex Additions	Shifting
Proposed Method	0	0	k_s
Method in Ref. [10]	$N/2 \odot \log_2 N$	$N \odot \log_2 N$	0

Here, k_s is the average of the Doppler estimation for the local carrier frequency acceleration described in Section III. From Table III, the complexity is reduced a lot since the processing of the shifting of the data for FFT calculation is trivial. Also the *N*-point FFT calculation is replaced with the *M N*/*M*-point FFT calculation, which cuts off some complexity too. Different from the algorithm in [4], the variable rate sampling is used in this algorithm for much more accurate carrier acquisition. Otherwise, the Doppler frequency will spread to a rather small range, which deteriorates the acquisition accuracy and affects the carrier recovery effect.

VI. CONCLUSIONS

In this paper, we have presented the associated two-stage carrier acquisition and tracking for high dynamic and weak satellite signals efficiently. In the first stage, the coarse carrier acquisition, mainly the estimation of the Doppler frequency and Doppler rate, is implemented by the FFT frequency domain cyclic shifting accumulation of the modified variable rate sampling periodogram method at a moderate complexity. In the second stage, a second-order FLL accompanied by a third-order PLL is designed to perform the carrier tracking and combat the residual carrier offsets after the compensation of the carrier offsets by their estimates from stage one under extremely low SNR and high dynamic environments. The simulation results show that the proposed method provides a rather precise carrier acquisition of frequency estimate of less than 20Hz at the cost of rather low complexity. And it can be further corrected by the self-feedback loop mechanism of the FLL-PLL even at extremely low SNRs. Therefore, the proposed carrier acquisition and tracking can be efficiently applied in the real time carrier synchronization of the satellite TT&C systems with good performance and low complexity.

REFERENCES

[1] M. Katayama, A. Ogawa, and N. Morinaga, "Carrier synchronization under Doppler shift of the nongeostationary satellite communication systems," in *Proc. Singapore ICCS/ISITA '92. 'Communications on the Move'*, Singapore, Nov. 1992, vol. 2, pp. 466-470.

[2] H. Meyr, M. Moeneclaey, and Stefan A. Fechtel, *Digital Communication Receivers: Synchronization, Channel Estimation and Signal Processing*, (1st Edition) New York, NY(USA): John Wiley&Sons, Inc., 1998, ch. 6, pp. 400-418.

[3] L. B. Jackson, D. W. Tufts, F. K. Soong, and R. M. Rao, "Frequency estimation by linear prediction," in *Proc. IEEE International Conference on Acoustics, Speech, and Signal Processing*, Tulsa, Oklahoma, USA, Apr. 1978, pp. 352-356.

[4] R. Duan, R. Liu , Y. Zhou, Q. Song, and Z. Li, "A carrier acquisition and tracking algorithm for high-dynamic weak Signal," in *Proc. 26th Conference of Spacecraft TT&C Technology in China vol.187 of the series Lecture Notes in Electrical Engineering*, Sep. 2012, pp. 211-219.

[5] Y. Li, H. Fu, P. Y. Kam, "Improved, approximate, time-domain ML estimators of chirp signal parameters and their performance analysis," *IEEE Transactions on Signal Processing*, vol. 57, no. 4, pp. 1260-1272, April 2009.

[6] H. Lu, W. Wang, and Q. Gu, "Carrier synchronization technique for low SNR and high dynamic condition," *Information and Control*, vol. 39, no. 4, pp. 451-454, Aug. 2010.

[7] F. D. Natal, "AFC tracking algorithm," *IEEE Transaction on Communications*, vol. 32, no. 8, pp. 935-947, Aug. 1984.

[8] W. Li, S. Liu, C. Zhou, S. Zhou, and T. Wang, "High dynamic carrier tracking using Kalman filter aided phase-lock loop," in *Proc. International Conference on Wireless Communications, Networking and Mobile Computing*, Shanghai, China, Sept. 2007, pp. 673-676.

[9] J. Miao, Y. Sun, J. Liu, and W. Chen, "A Kalman Filter Based Tracking Loop in Weak GPS Signal Processing," in *Proc. FSKD '09. Sixth International Conference on Fuzzy Systems and Knowledge Discovery*, Tianjin, China, Aug. 2009, vol. 4, pp. 438-442.

[10] E. Satorius, P. Estabrook, J. Wilson, and D. Fort, "Direct-to-earth communications and signal processing for Mars exploration rover entry, descent, and landing," *JPL INP, Tech. Rep.*, pp. 1-35, Mar. 2003.

[11] V. A. Vilnrotter, S. Hinedi, and R. Kumar, "Frequency estimation techniques for high dynamic trajectories," *IEEE Transactions on Aerospace and Electronic Systems*, vol. 25, no. 4, pp. 559-577, Jul. 1989.

[12] S. Hinedi and J. LStatman, *High-Dynamic GPS Tracking--Final Report*, JPL Publication, Dec, 1988.

[13] S. Ma, J. Jiang, and Q. Meng, "A fast, accurate and robust method for joint estimation of frequency and frequency rate," in *Proc. International Symposium on Intelligent Signal Processing and Communications Systems*, Chiang Mai, Thailand, Dec. 2011, pp. 1-6.

[14] X. Pan, "ALE-FFT algorithms for weak signal acquisition," in *Proc. International Symposium on Intelligent Signal Processing and Communication Systems*, Chengdu, China, Dec. 2010, pp. 1-4.

[15] Z. Yang, L. Yu, Q. Ding, S. Kang, and M. Han, "Research on QPSK carrier synchronization algorithm based on software defined radio," in *Proc. Third International Conference on Robot, Vision and Signal Processing*, Kaohsiung, Taiwan, China, Nov. 2015, pp. 276-279.
[16] T. Fan, X. Wang, and B. Zheng, "A novel carrier synchronization method for SOQPSK signal in satellite communication," in *Proc. International Conference on Information and Communications Technologies*, Nanjing, China, May 2014, pp. 1-5.
[17] Q. Huang, H. Xu, J. Yu, and H. Zheng, "Parameters adjusting of third-order PLL used in LEO mobile satellite communication systems," in *Proc. 17th International Conference on Advanced Information Networking and Applications*, Xi'an, China, Mar. 2003, pp. 464-467.
[18] D. Y. Abramovitch, "Analysis and design of a third order phase-lock loop," in *Proc. IEEE Military Communications Conference*, San Diego, CA, USA, Oct. 1988, vol. 2, pp.455-459.
[19] F. M. Gardner, *Phaselock Techniques*, 3rd ed., Hoboken, NJ(USA): John Wiley & Sons, 2005, ch. 11, pp. 283-326.
[20] A. V. Oppenheim, W. S. Ronald, and R. B. John, *Discrete-Time Signal Processing*, 3rd ed., Englewood Cliffs, NJ(USA): Prentice hall, 2009, ch. 9, pp. 693-718.

Xiang Gao received his B.S.E.E and M.S.E.E degree from Harbin Institute of Technology in 1997, and from Beijing Institute of Technology in 2005, respectively. He is currently pursuing his Ph.D. degree in E.E. from the School of Electronic and Information, Northwestern Polytechnical University (NWPU), Xi'an, China. His research interests include digital signal processing with its applications, the design and development of high speed real time DSP systems and so on.

Yong Li received his Ph.D., M.S., and B.S. degrees in Information Electronics and Systems from NWPU, China in 2005, 1988 and 1983 respectively. He is a professor of the School of Electronics and Information at NWPU. His research interests include digital signal processing with its applications, the design and development of high speed real time DSP systems, the cognitive radio and the software defined radio, *etc*.

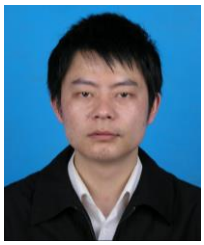

Jianrong Bao received his B.S. degree in Polymer Materials & Eng., and the M.S.E.E. degree from Zhejiang University of Technology, Hangzhou, China, in 2000 and 2004, respectively. He received his Ph.D. degree in E.E. from the Department of Electronic Engineering, Tsinghua University, Beijing, China, in 2009. He is with the School of Communication (Information) Engineering, Hangzhou Dianzi University, Hangzhou, China. His research interests include space wireless communications, modulation & demodulation, synchronization, channel coding, *etc*.